Original Study

Pasquale Acquafredda*, Felice Larocca, Antonella Minelli, Mauro Pallara, Francesca Micheletti

Petroarcheometric Analysis on Obsidian Artefacts Found Within Some Neolithic – Eneolithic Period Caves of Southern Italy

Abstract: In the last twenty years, obsidian artefacts have been found in important and often extensive karst cavities in Southern Italy: three located in Calabria (Grotta della Monaca, and Grotta del Tesauro, in Sant'Agata di Esaro, Cosenza; Grotta Pietra Sant'Angelo in San Lorenzo Bellizzi, Cosenza), one in Puglia (Grotta di Santa Barbara in Polignano a Mare, Bari) and another in Campania (Grotta di Polla, Salerno). All these sites, that have returned a total of 151 obsidian tools, were connected to human frequentation of the underground environments that occurred during the Holocene, which can be precisely located in the vast period between the Neolithic and the Eneolithic (6th–4th millennium BC). They are mainly blades and bladelets, but also burins together with scrapers and cores, generally of small dimensions. SEM-EDS and WD-XRF absolutely non-destructive analyses carried out on these items have shown that all samples have a source area in the obsidian outcrops of the island of Lipari (Messina, Italy). These data confirm that the Aeolian island of Lipari furnished the privileged obsidian extraction outcrops for most of the Neolithic and Eneolithic archaeological sites of Southern Italy.

Keywords: obsidian provenance, prehistoric caves, Southern Italy, SEM-EDS, WD-XRF, non-destructive analyses

1 Introduction

Source determination of obsidians artefacts is one of the main targets of petroarchaeometric research; it has been developed since the 1930s through partially destructive or absolutely non-destructive analytical

*Corresponding author: Pasquale Acquafredda, Dipartimento di Scienze della Terra e Geoambientali, via Orabona 4, Università degli Studi di Bari Aldo Moro, Bari, Italy; Centro Interdipartimentale, Laboratorio di Ricerca per la Diagnostica dei Beni Culturali, via Orabona 4, Bari 70125, Italy, E-mail: pasquale.acquafredda@uniba.it
Mauro Pallara, Francesca Micheletti, Dipartimento di Scienze della Terra e Geoambientali, via Orabona 4, Università degli Studi di Bari Aldo Moro, Bari, Italy
Felice Larocca, Centro Regionale di Speleologia "Enzo dei Medici" – Commissione di ricerca per l'Archeologia delle Grotte, via Lucania 3, 87070 Roseto Capo Spulico (CS), Italy; Centro di ricerca speleo-archeologica – Laboratorio di Paletnologia, via Pisani 26, 87010 Sant'Agata di Esaro (CS), Italy
Antonella Minelli, Dipartimento di Scienze Umanistiche, Sociali e della Formazione, via De Sanctis, Università del Molise, Campobasso, Italy

techniques useful for the characterization of lithic materials.

Below, in chronological order, are reported the papers relating to each procedure and also those that have improved their results in more recent times.

Among the pioneering research, Wainwright in 1927 proposed the determination of refraction index and density of obsidian artefacts for their archaeometric characterization; successively other techniques were used, for provenance determination of obsidian artefacts, like optical emission spectroscopy (Cann & Renfrew, 1964); instrumental neutron activation analysis (Gordus, Wright, & Griffin, 1968); fission track dating (Bigazzi, Bonadonna, Belluomini, & Malpieri, 1971); energy and wavelength dispersive X-ray fluorescence using peak intensity ratios of various elements (Nelson, D'Auria, & Bennett, 1975; De Francesco, Crisci, & Bocci, 2008, respectively); particle induced X-ray emission (Nielson, Hill, Mangelson, & Nelson, 1976); electron microprobe (Merrik & Brown, 1984); inductively-coupled plasma mass spectrometry (ICP-MS), with or without laser ablation (Tykot & Young, 1996 and Gratuze, 1999, respectively); gamma rays (Shackley, 1998); scanning electron microscopy coupled with energy dispersive spectrometer (Acquafredda, Andriani, Lorenzoni, & Zanettin, 1999); electron spin resonance (Duttine, Villeneuve, Poupeau, Rossi, & Scorzelli, 2003); Mössbauer spectroscopy (Stewart et al., 2003); Raman micro-spectroscopy (Bellot-Gurlet, Le Bourdonnec, Popeau, & Dubernet, 2004); portable or handheld portable energy dispersive spectrometers (Phillips & Speakman, 2009; Frahm, Doonan, & Kilikoglou, 2014 respectively) and recently laser-induced breakdown spectroscopy (Syvilay, Bousquet, Chapoulie, Orange, & Le Bourdonnec, 2019).

During the past 25 years, a systematic programme for determining obsidian provenance at the Dipartimento di Scienze della Terra e Geoambientali of Bari University, has provided a well-defined outline of the various geological derivation outcrops (Acquafredda et al., 1999; Acquafredda & Paglionico, 2004; Acquafredda, Muntoni, & Pallara, 2018; Acquafredda, 2019). Moreover, in the last two decades, from 2000 to 2018, an intense activity of exploration of archaeological deposits in caves was carried out in close collaboration between the Università degli Studi di Bari Aldo Moro (Bari, Italy), the Centro Regionale di Speleologia "Enzo dei Medici" (Cosenza, Italy) and the Università del Molise (Campobasso, Italy).

This paper presents the results of an archaeometric research carried out on 151 fragments of obsidian, collected in five different caves of Southern Italy (Fig. 1): Grotta della Monaca, (54 obsidian artefacts), Grotta del Tesauro, (11 obsidian artefacts), Grotta Pietra Sant'Angelo (46 obsidian artefacts), Grotta di Santa Barbara (54 obsidian artefacts) and Grotta di Polla (6 obsidian artefacts).

Obsidian samples were investigated with regard to their typological and functional use; their source area has also been characterized in an absolutely non-destructive way using WD-XRF and SEM-EDS techniques.

2 The Speleo-archaeological Sites

The caves that form the basis of this study are located in three distinct regions of Southern Italy: Puglia, Campania and Calabria (Fig. 1). In Puglia can be found the Grotta di Santa Barbara (municipality of Polignano a Mare, province of Bari); in Campania the Grotta di Polla (municipality of Polla, province of Salerno); in Calabria, the Grotta di Pietra Sant'Angelo (municipality of San Lorenzo Bellizzi, near Cosenza) together with the Grotta della Monaca and the Grotta del Tesauro (the latter both in the municipality of Sant'Agata di Esaro, province of Cosenza).

All the cavities examined are of natural origin and develop into limestones or carbonate low grade metamorphic rocks, with planimetric developments varying from a few tens of meters (Pietra Sant'Angelo and Tesauro) to several hundred (Santa Barbara and Monaca) up to over a kilometer (Polla). The explorations of the internal archaeological sites took place over the last twenty years, by the Università degli Studi di Bari Aldo Moro, the Università del Molise and the Centro Regionale di Speleologia "Enzo dei Medici".

From North to South, the first site you can visit is Grotta di Santa Barbara (Fig. 1), which opens along the central part of the Puglia shoreline, at an altitude of about 50 meters above sea level, at a very short distance from the Adriatic Sea.

The Grotta di Santa Barbara (40°58'13.6"N, 17°14'32.3"E) is an interlayer cave, formed into the limestones belonging to the Calcare di Bari Formation, Upper Triassic in age.

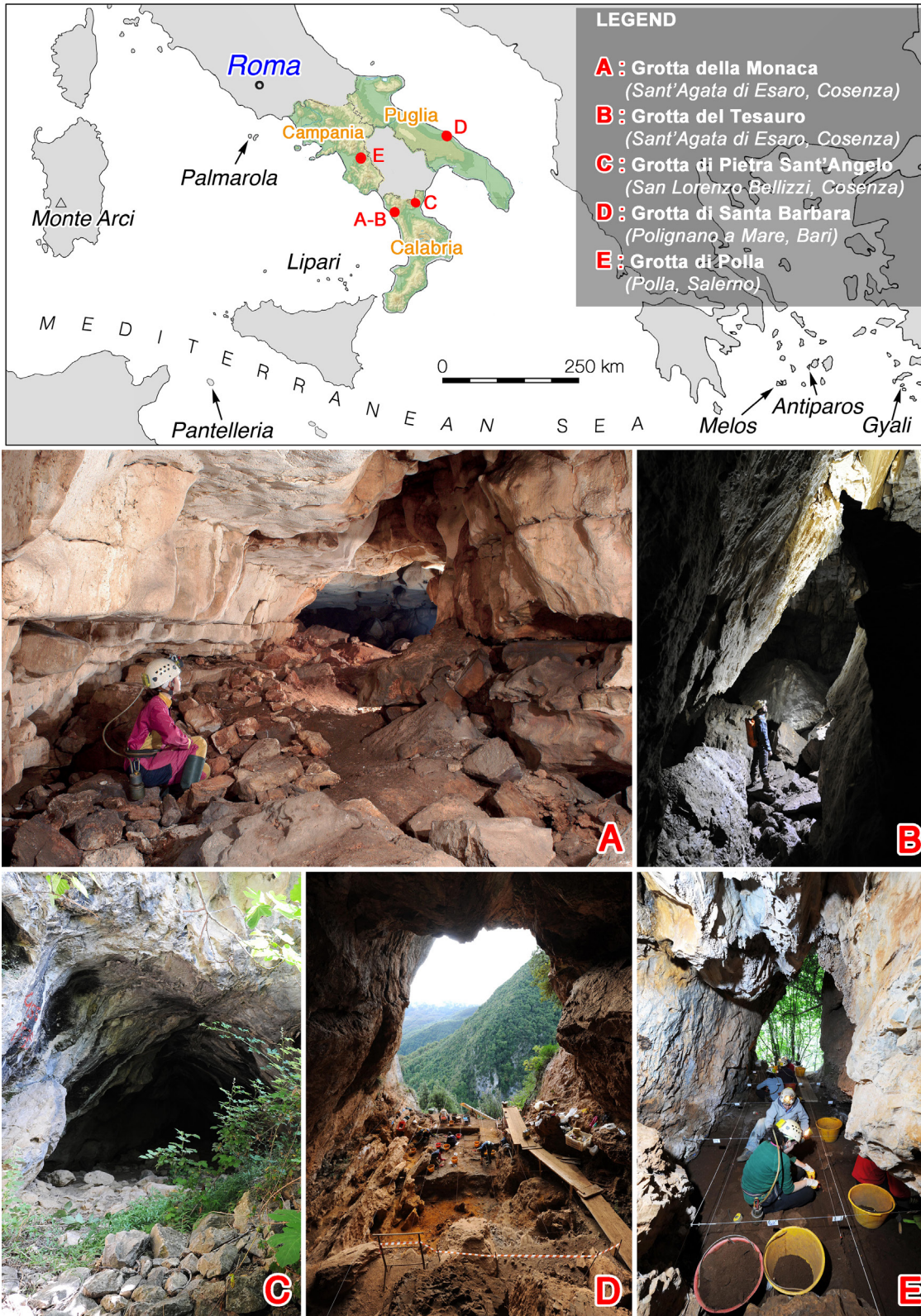**Figure 1:** Studied archaeological sites and Mediterranean obsidian source area. In black is the name of the central-eastern Mediterranean source area. The geographic position in Southern Italy of the studied karst cavities and the relative photographs are indicated with an uppercase red letter (photographs by F. Larocca); in orange are specified the Southern Italy province which house the karst cavities.

Its development, equal to 700 meters, is divided into a long main course with short lateral branches. The cavity was intensely frequented during the Neolithic age also because it was integrated into an extended outdoor village relevant to the same chrono-cultural phase. The reasons for the ancient human presence within the cave are probably connected to the sphere of worship, as various archaeological evidences (pottery ware and valuable objects, animal offerings, etc.) seem to demonstrate. However, there are also funerary attestations, with remains of individuals buried in the cavity. The excavations recovered 54 obsidian artefacts from Middle-Late Neolithic contexts, as confirmed by radiocarbon dating which gives ages between 5000 and 4500 BC (Larocca, 2017; Acquafredda & Larocca, 2017).

Moving to the East, on the Tyrrhenian side of the Italian Peninsula, the second studied site that returned obsidian is the Grotta di Polla in Campania (40°30'36.4"N, 15°29'17.6"E), not too far from the Alburni Mountains (Fig. 1). This cavity formed into limestones, Triassic in age, is currently still in the process of exploration and archaeological excavation; it opens up at the Northern outlet of the so-called "Vallo di Diano", a large flat tectonic depression (*graben*) in which it is possible to recognize the remains of an ancient Pleistocene lake. The cave is over a kilometer long and with enormous underground rooms; it has a registered human presence from the end of the Neolithic to the classical age. Recent excavations have highlighted a burial area from which 6 obsidian artefacts derive, whose general chronological context can be fully placed in the Eneolithic (Gastaldi, 1974; Minelli & Larocca, 2019).

The last three underground sites examined are located in Calabria. The first of these, the Cave of Pietra Sant'Angelo (39°52'26.0"N, 16°20'42.7"E), is a cavity whose exploration has recently begun and is still in progress (Fig. 1). The aperture evolves into the meta-limestones, Lower Oligocene in age, of the Frido Unit and is located on the Eastern slope of the Pollino mountain massif, not far from the Ionian Sea. It develops for just under 20 m and was the site of an important prehistoric settlement at high altitude, at about 850 m above sea level (Larocca, Minelli, & Larocca, 2019). Archaeological excavations have returned 46 artefacts in obsidian, referable to the Neolithic and Eneolithic ages. The reasons for human frequentation of this cavity that is also comfortable, widely illuminated by daylight and well exposed to the South, seem to be basically residential; recently also a human burial has been found, whose radiocarbon dating gives an age of 4992 ± 92 (1 σ) annum BC.

Moving toward the Tyrrhenian side of Calabria, just to the West, the upper valley of the Esaro River can be reached, where the last two sites are located: Grotta della Monaca (39°37'39.5"N, 15°58'31.9"E) and Grotta del Tesauro (39°37'29.9"N, 15°58'20.2"E).

Both the cavities develop into the impure meta-limestones of the San Donato Unit, Triassic in age; the limestones often are particularly rich in iron and copper assuming an evident banded texture. The presence of high concentrations of iron and copper has led to the formation of abundant mineralizations represented essentially by goethite [FeO(OH)], malachite [$Cu_2CO_3(OH)_2$] and azzurrite [$Cu_3(CO_3)_2(OH)_2$].

The Grotta della Monaca cavity, over half a kilometer long, was intensely frequented by man from the upper Paleolithic to the Middle Ages, for a total duration of about 20,000 years (Fig. 1). The reason for such a long-term human use of this cave is arguably due to the internal abundance of iron and copper mineralization, objects of mining throughout the millennia. Only during the middle Bronze Age was the cavity also used as a sepulchral site, receiving dozens of burials (Larocca, 2010, 2012). The 54 artefacts in obsidian from the cave all derive (apart from a single specimen) from the front of the underground system, to immediate contact with the surface, and refer to both the Neolithic and Eneolithic ages. The Grotta del Tesauro cavity, is located on the opposite side of the same valley where Grotta della Monaca opens up and it develops for only about 60 meters (Fig. 1). The cave is rich in iron mineralization and for this reason hosted mining activities in the Eneolithic age and successively also in the post-medieval period (Larocca & Breglia, 2014). The 11 artefacts in obsidian recovered from the excavations carried out in the antechamber (the parts of the cavity in direct contact with the surface and therefore reached by natural light) are all related to the Eneolithic age.

3 Archaeological Characterization

The 151 obsidian artefacts from the five caves comprised both tools and waste material. The most represented tools are the blades and the lamellae (Fig. 2a – 2d), which in many cases had to be inserted and be part of more complex tools made of organic material (wood, bone, antler, etc.), which did not survive. Although in absolutely limited quantities, there are also burins (obtained by blades or splinters, Fig. 2e) and small scrapers. The nuclei are rare, mostly of small dimensions (indicating an extreme exploitation of the raw material) and only exceptionally of medium size (Fig. 2f – 2g). The splinters, frequent in the examined underground contexts, sometimes indicate the presence of lithic workshops on site, sometimes simple actions to revive the functional margins of the instruments as well as the preparation of nuclei. The chronological horizon pertaining to all the analysed instruments is between the middle Neolithic and the entire chronological period of the Eneolithic (5th–3rd millennium BC). During the Bronze Age, of which there are various and often important attestations in some of the treated cavities (such as Grotta della Monaca), the use of obsidian seems to have been almost completely abandoned in favor of other lithic materials. The diminution in obsidian artefacts in the Bronze Age has also been confirmed in western Mediterranean sites (Freund & Tykot, 2011); conversely, significant use of obsidian is attested in the Aegean area in the Bronze Age (Carter & Kilikoglou, 2007).
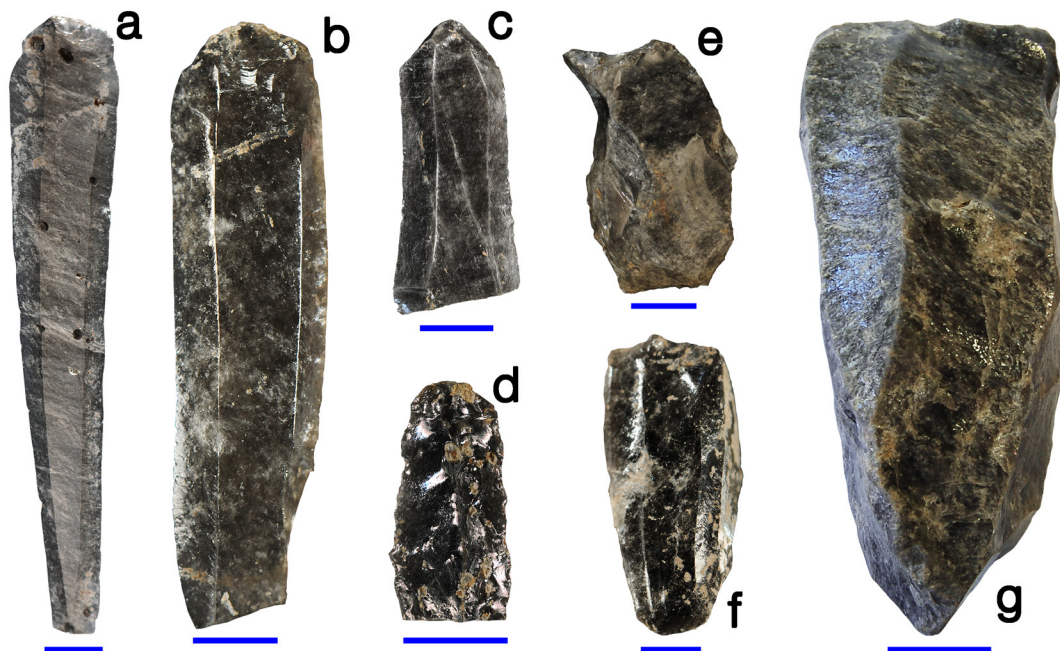
Figure 2: Photographs of the obsidian finds from the underground examined karstic sites; **a–d**: flakes and blades, intact and fragmentary (**a–b** from Grotta di Santa Barbara; **c–d** from Grotta del Tesauro); **e**: punch on splinter from Grotta della Monaca; **f–g**: cores for detachment of slats and blades (**f** from Grotta di Santa Barbara; **g** from Grotta di Polla) (photographs by F. Larocca & A. Di Meo). Blue scale bar is 1 cm.

The obsidian finds, indicating the use of the relative instruments in daily activities of various types (Monaca, Tesauro, Pietra Sant'Angelo), are generally more abundant in the antechamber of the caves; in particular cases they also appear in rather internal sectors of the cavities, where they can be set in the context of rituals connected to sacral or sepulchral necessity (Santa Barbara and Polla).

It is important to highlight that the obsidian finds from the five studied caves demonstrate a wide use of this raw material among the chipped stone instruments of the people who frequented the distinct

underground sites. Obsidian is associated with flint during the Neolithic until it became an almost exclusive raw material in the final stages of this era and the following Eneolithic age: this aspect emerges in all its evidence in the caves object of our study, each characterized by important phases of anthropic frequency between Neolithic and Eneolithic. The investigated stratigraphies have returned both splinters and instruments. In order to understand their relationships and their respective quantitative relationships, typological analysis, the study of underground spatiality and the function performed by the various parts of the cavities during prehistoric frequentation, is very important.

In general, a high number of splinters are recognized in the cavity sectors in which various types of activities, including specialized ones, were carried out frequently, which required the use of obsidian. This was done in particular at the entrances or in their immediate vicinity (antechamber), so as to ensure the advantage of natural surface lighting without resorting to artificial lighting systems. This is what is observed, for example, in Grotta della Monaca, in Grotta di Pietra Sant'Angelo and in Grotta del Tesauro. In all these sites, almost all of the obsidian finds, except in exceptional cases, derive from the areas of the antechamber. The more or less abundant presence of splinters indicates, depending on the cavities, various actions such as i) reviving the cutting edges of the instruments, shaping work and particular preparation of the raw material (for example, preparing the cores), ii) the presence of real lithic workshops on site (but only when the number of splinters is high), iii) accidental breakages due to use or even to post-deposition events (for example trampling or knocks).

The instruments can be found in association with the splinters or not; when their abandonment or intentional deposition does not clearly emerge, they may constitute the result of a loss or temporary provision, for subsequent reuse, for example, which is not followed by recovery for reuse. It should not be forgotten, however, that many obsidian instruments must have been originally handled in organic materials (wood, bone, horn, etc.), which were not received because they deteriorated or from which they separated over the millennia: therefore it will be good to imagine what we define obsidian "tools" as being part of more complex and articulated tools (for example sickles, rudimentary knives, arrows, etc.).

The splinters, therefore, except for rare cases, are almost completely absent in the deepest and most distant underground sectors, generally obscure. Here it is more common to find instruments intact or fragmented. This is evident from the research carried out at Grotta di Polla and Grotta di Santa Barbara, where obsidian tools were found only far from the entrance of the cave. In the first cavity, the instruments (a nucleus and some fragmentary blades) were part of a sepulchral context and, with all evidence, had been placed at the same time as the deceased, perhaps as gifts or as part of rituals unknown to us. In Grotta di Santa Barbara, on the other hand, obsidian tools (especially long and thin bladelets, with a splendid workmanship) were found in areas with a clear cult destination, as evidenced by the association with other valuable materials (terracotta pots, lanterns and lithic axes, as well as offerings of wildlife). The perfect state of conservation of these obsidian artefacts, in the case of Santa Barbara, highlights their certainly intentional non-use.

The reduced number of obsidian finds found in caves and caverns, compared to the much greater quantities attested at surface sites, is certainly due to several factors that may be summarised as: i) these sites are generally more difficult for human acquaintances that have not been aimed at particular uses, ii) the minority number of investigations and excavation campaigns carried out in the subsoil compared to those carried out on the surface, in turn a consequence of the limited number of teams that specifically deal with speleo-archaeological research.

4 Petroarchaeometric Investigations

The obsidian artefacts were characterised using two different non-destructive techniques: i) Scanning Electron Microscopy coupled with an Energy Dispersive spectrometer (SEM-EDS) and ii) wavelength dispersive X-ray fluorescence (WD-XRF) using peak intensity ratios of some trace elements.

Both of the different techniques are able to establish the geological source of the artefacts.

The SEM-EDS equipment (Fig. 3) makes it possible to determine the glass (major and minor elements)

and microphenocrysts composition of the obsidian artefact; these results can be easily compared with those of other laboratories using similar instrumentation or different techniques such as EPMA, PIXE (Acquafredda & Muntoni, 2008), LA-ICP MS, INAA.
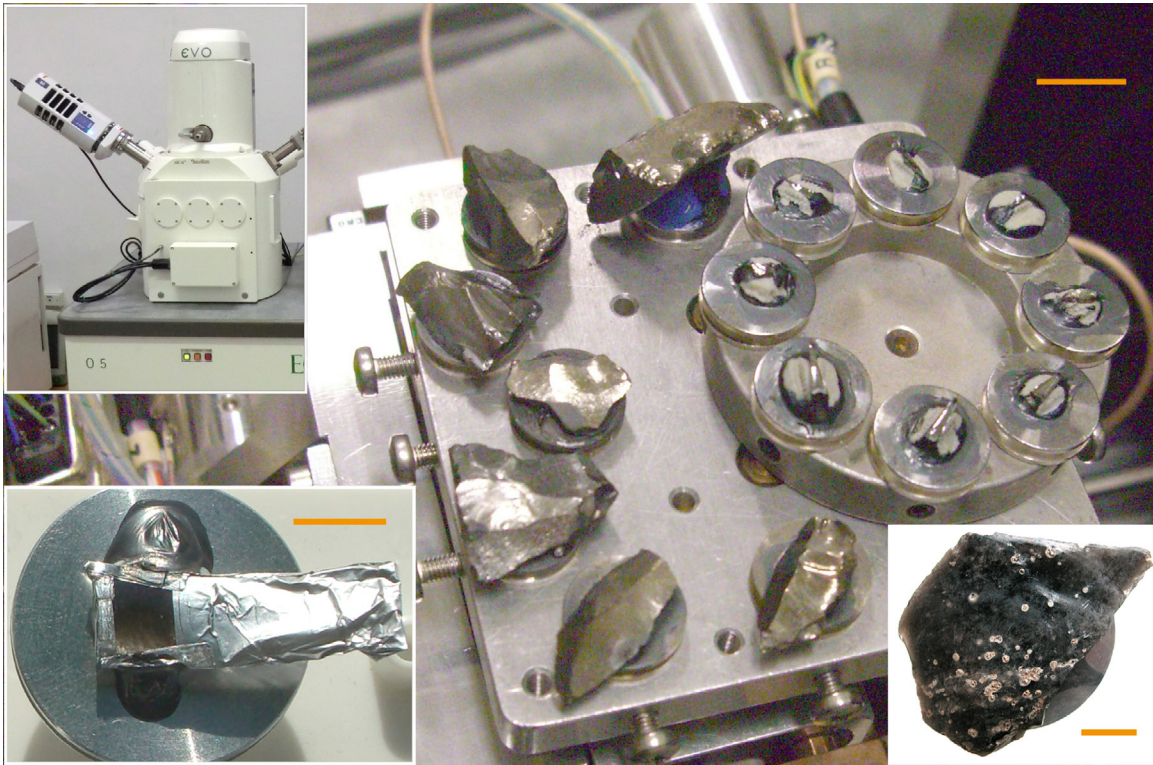

Figure 3: SEM-EDS analyses; up to 15 artefacts can be mounted on the sample older using plasticine (in blue color), silicone material (in grey color), conductive tape or colloidal graphite (in black color). In the left upper part of the figure is a photograph of the SEM column; on its left side the X-ray detector. In the left lower part of the figure an obsidian bladelet protected with an aluminium paper to avoid that the carbon film can cover the entire surface of the sample. In the right lower part of the figure is an obsidian particularly rich in analcimised spherulites (sample L 161 from Grotta della Monaca). Orange scale bar is 1 cm.

SEM-EDS can be used to characterize specimens whose length varies from a few micrometers up to 15 cm but is necessary for the sample, or part of its surface, to be sputtered with carbon before the analysis; the carbon film can be easily removed at the end of the investigation using either acetone or ethyl alcohol.

By contrast, the WD-XRF technique using peak intensity ratios is particularly useful for obsidian samples that are difficult to analyse with other methodologies like SEM-EDS or LA-ICP MS because their surface is slightly altered or covered by a thin carbonate film or has a pumice texture (Acquafredda & Muntoni, 2008; Acquafredda, Muntoni, & Pallara, 2013, 2018). Moreover, the WD-XRF technique (Fig. 4) is very rapid, about 20 minutes per sample and sufficiently inexpensive.

The measurements obtained by WD-XRF can be compared only with other WD-XRF values produced in other research laboratories, with the only restrictions that X-ray intensities must be measured as background and interference free (Appendix – Table 1) and on samples with dimensions ranging from 5 mm to 5.15 cm (Acquafredda et al., 2018).

Normally, before SEM investigations the obsidian sample must be washed in an ultrasonic bath with acetone or absolute ethyl alcohol. Any carbonate incrustations covering the surface of the sample can be easily removed by immersing the specimen in cold acetic acid for at least 24 hours (Acquafredda & Muntoni, 2008).

In some cases the acetic acid treatment must be extended up to 12 days to remove completely the carbonate films. Alternatively a very small part of the obsidian archaeological sample can be cutted obtaing a fresh surface, free from alterations and concretions.
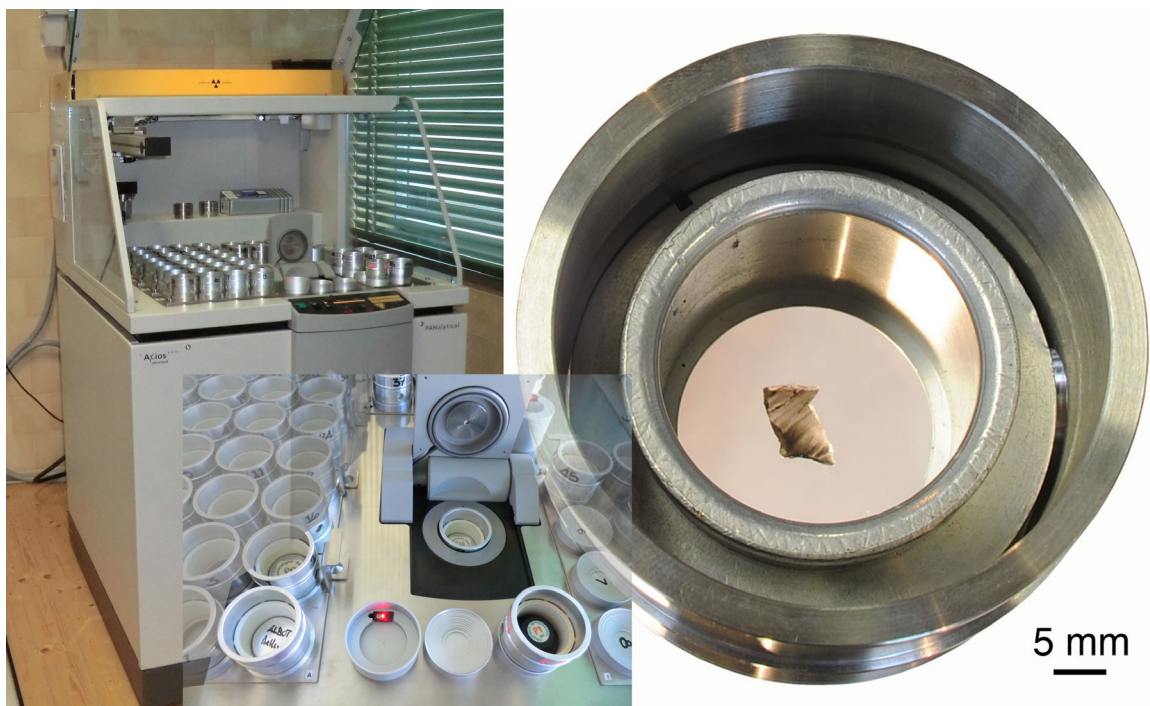
Figure 4: WD-XRF spectrometer used for chemical characterization of the obsidian samples. The spectrometer can accommodate up to 48 specimen holders; on the right the detail of one sample holder closed at the base by a thin sheet of Mylar© in the center of which is placed a very small obsidian artefact which seems suspended in the air.

After cleaning treatments, the obsidian is fixed on an aluminium support (stub), orienting part of its concave or convex surface as much as possible parallel to the surface of the stub; to properly orient the sample it is possible to use pieces of paper or plastic supports (plasticine, silicone materials) that do not degrade under high vacuum or in contact with the electron beam of the SEM (Fig. 3).

Once the obsidian is properly positioned, its surface is sputtered with a 30 nm thick carbon film. If the sample presents a pumice texture, spherulites (often analcimised, Fig. 3), or particularly delicate parts, these portions can be protected with a thin covering film (an aluminium foil sheet for food is sufficient) fixed with adhesive conductive tape (aluminium or copper tape); finally, one drop of colloidal graphite will close the electrical bridge between the surface of the specimen and the stub (Fig. 3).

The glass analyses of obsidian artefacts (Appendix – Table 2) were performed using a Zeiss-Leo EVO50XVP scanning electron microscope coupled with an X-max (80 mm^2) Silicon drift Oxford detector equipped with a Super Atmosphere Thin Window ©; the operating conditions were: 15 kV accelerating potential, 500 pA probe current, about 25,000 output cps as average count rate on the whole spectrum, counting time 50 s and 8,5 mm working distance. X-ray intensities were converted to the concentration of the element using the XPP correction scheme, developed by Pouchou & Pichoir (1988, 1991), granted as quantitative software support by Oxford-Link Analytical (U.K.). The microanalytical data were checked against numerous reference materials (standards from Micro-Analysis Consultants Ltd.). Analytical precision was 0.5% for concentrations > 15 wt.%, 1% for concentrations of about 5 wt.%, and < 15% for concentrations near the detection limit. Given the analysed composition, the 1σ precision corresponded to the following values: SiO_2 = 0.10−0.20 wt.%, TiO_2 = 0.08−0.10 wt.%, Al_2O_3 = 0.08−0.13 wt.%, FeO = 0.05−0.15 wt.%, MnO = 0.04−0.6 wt.%, MgO = 0.08−0.13 wt.%, CaO = 0.04−0.14 wt.%, Na_2O = 0.04−0.06 wt.% and K_2O = 0.04−0.12 wt.%; two of the standards used for element calibrations (augite and orthoclase) are reported in Table 3 (see Appendix).

The obsidian samples whose surface was particularly altered, to the extent that it did not permit the glass SEM analysis, were characterized with the WD-XRF technique using a PANalytical AXIOS-Advanced XRF spectrometer, equipped with a 4 kW Rh super sharp end window X-ray tube. The peak intensity ratio of

trace elements such as Rb, Sr, Y, Zr and Nb, that are contiguous in the Periodic Table of Elements, provides accurate information on the obsidian source area (De Francesco, Bocci, & Crisci, 2011; Acquafredda et al., 2018). The X-ray intensities of these trace elements were measured under the following operating conditions of the XRF spectrometer: X-ray tube power supply 60 kV and 66 mA; scintillator detector to collect the X-ray lines dispersed by a LiF 220 crystal (Acquafredda et al., 2018).

The developed procedure does not require any preventive treatment of the sample and is preferably used when the specimens are covered by thin carbonate incrustations or are very rich in pores or in spherulites, often analcimised. For the X-ray measurements, obsidian artefacts whose length must not exceed 5.15 cm were gently positioned in the middle of a thin sheet of Mylar© (Fig. 4) which is perfectly transparent to the detected X-rays lines (Rb, Sr, Y, Zr and Nb Kα lines), used to close the XRF spectrometer sample holder below (Acquafredda et al., 2018). The X-ray intensity ratios measured (Appendix – Table 1) were compared with the literature data on different geological obsidian sources of the Mediterranean basin (Acquafredda et al., 2018, 2019).

5 Comments on Analytical Results

SEM-EDS and WD-XRF absolutely non-destructive analyses carried out on these items showed as all samples are referable to the obsidian outcrops of the Lipari Aeolian Island (Messina, Italy). These data confirm that in peninsular Southern Italy the most widespread obsidian is the one traded from Lipari (Acquafredda, Larocca, Muntoni, & Pallara, 2016; Acquafredda, Muntoni, & Pallara, 2017; Tykot, 2017; Freund, 2018).

The choice of the analytical technique, SEM-EDS or WD-XRF, in some cases depended on the state of alteration of the sample but more often on the instrumentation at that moment being more available or at that moment functioning: it should be remembered that the analyses were carried out following the excavations in the karst cavities, over a very long period of time lasting about two decades. The choice of the instrumentation sometimes depended on what was currently working since often the scarce financial resources do not allow the repair of the instrumentation even for periods of more than one year.

SEM-EDS determinations were carried out on the glass of the samples; each determination obtained is the arithmetic mean of at least 3 microanalysis in three different points of the sample surface (the samples indicated as "untreated samples" in figure 5) carefully avoiding the micro-crystals and those parts where BSE images indicate the presence of spherulites, carbonate films or a particularly altered surface. In cases where the sample is completely covered by fine carbonate encrustation that does not allow a correct determination of the composition of the glass (samples indicated in orange in figure 5: 152 and 163 of the Grotta della Monaca site and 28 and 133 of the Grotta di Santa Barbara site), the obsidian artefacts were treated by immersing them in cold acetic acid for a minimum of 72 hours up to 12 days. In some cases the treatment with acetic acid was sufficient to completely remove the carbonate incrustations (sample indicated in purple in figure 5: 28 and 133 from the Grotta di Santa Barbara site), in other cases (sample indicated in purple in figure 5: 152 and 163 from the Grotta della Monaca site) a very small fragment (a few millimeters) of the sample was detached to analyse its internal fresh surface (sample indicated in green in figure 5: 152 and 163 of the Grotta della Monaca site).

The petroarchaeometric analyses carried out on obsidian artefacts found in the different caves investigated, attest a derivation of the raw material from Lipari Island. This confirms a diffusion model already highlighted from previous research carried out in several archaeological sites in Southern Italy. A direct passage of the raw material from the Aeolian archipelago to the coasts of Calabria has been proved. Following various directions developing both along the coast and through the internal valleys, the Aeolian obsidian artefacts were traded toward the North, reaching the close-by territories of Basilicata, Campania and Puglia and, in many cases, even beyond. Therefore, these volcanic rocks are a non-local product, which were carried from the outside, unlike many other rocks, used for artefact realisation, for which petroarchaeometric characterizations found source areas not far from the sites. On the contrary, in addition to obsidians artefacts and referring to the five sites reported in this paper, only at Grotta di Santa Barbara (Polignano a Mare, Bari) did other used exotic rock (such as quarzarenites and mixed arenites) come from

distances greater than 100 km (Acquafredda & Larocca, 2017).
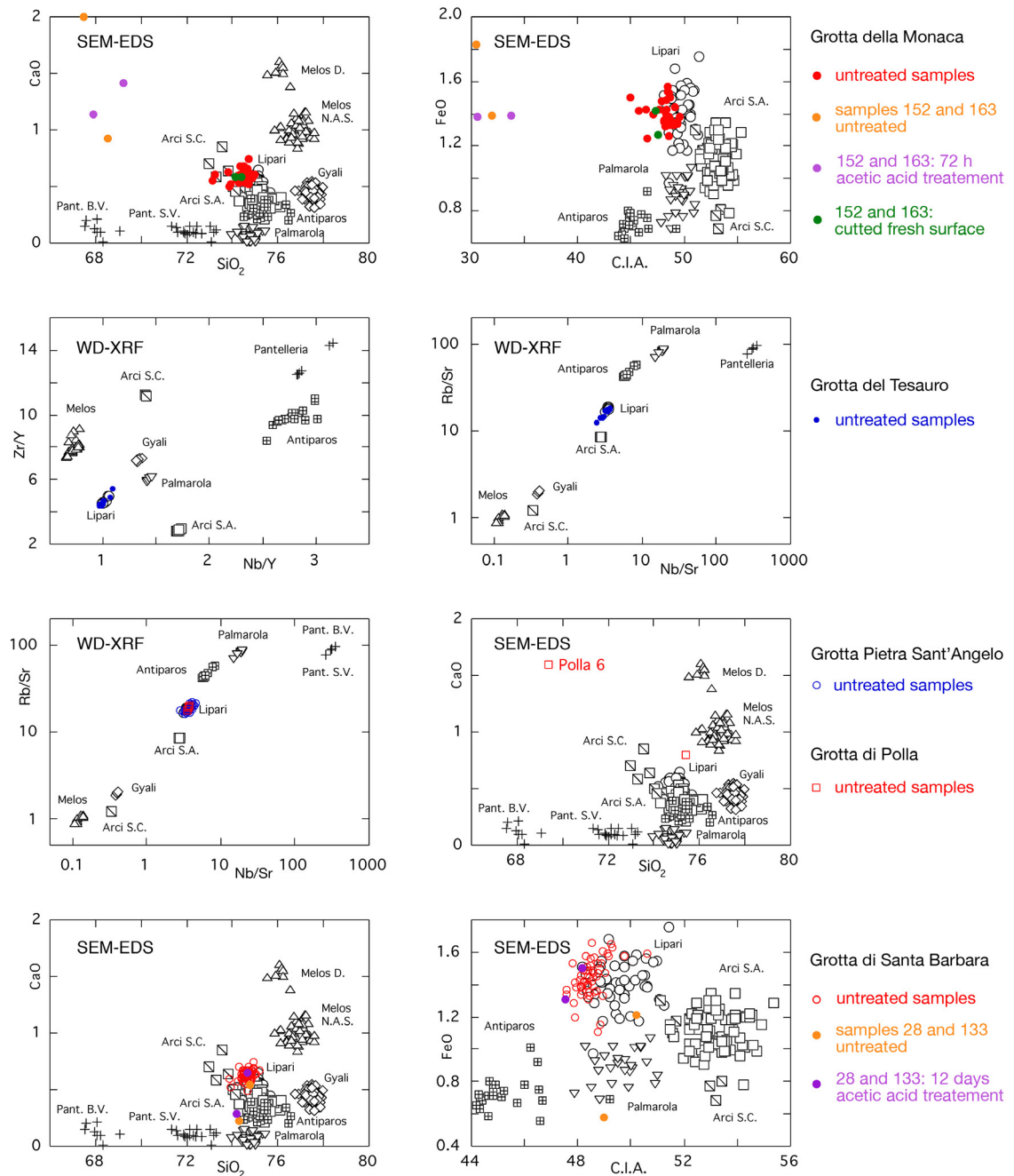
Figure 5: Plots of the SEM-EDS and WD-XRF X-ray analyses of obsidian artefacts collected in the five studied karst archaeological sites (Grotta della Monaca, Grotta del Tesauro, Grotta Pietra Sant'angelo, Grotta di Polla and Grotta di Santa Barbara) present in Southern Italy; for the explanation of the sample treatment see text. The literature data on different geological obsidian sources of the Mediterranean basin are from Acquafredda et al., 1999, 2018, 2019. Sub-sources outcrops: Monte Arci, S.C. = Perdas Urias; S.A. = Conca Cannas, Canale Perdera and Riu Solacera. Pantelleria, B.V. = Bagno di Venere, S.V. = Salto la Vecchia and Balata dei Turchi. Melos, D. = Demenegaki; N.A.S. = Nihia, Adamas and Sarakiniko. C.I.A. = Chemical Index of alteration $[Al_2O_3/(Al_2O_3 + CaO + Na_2O + K_2O)$ in mol.%].

6 Conclusions

Obsidian is one of the most used lithic materials by man in ancient times together with flint. Its importance is demonstrated by the fact that it, even with respect to flint, represents one of the most exotic and therefore often imported materials found in Neolithic and Eneolithic sites such as those of the studied cavities (Grotta della Monaca, Grotta del Tesauro, Grotta Pietra Sant'Angelo, Grotta di Santa Barbara, Grotta di Polla) present in Southern Italy.

The obsidian of these five sites was traded from the island of Lipari. The exclusive identification of the source area with Lipari may depend on the representative quantity of the excavated samples which may not be numerous enough due to lack of a large number of archaeological teams investigating the subsoil cavity.

More likely the preponderant origin of the raw material from the Aeolian Islands is due to the geographical proximity of the Aeolian archipelago to the Calabrian coasts from which the precious black volcanic glass, through the internal valleys and the different coasts, then spread to most of the southern sector of the Italian Peninsula.

References

Acquafredda, P. (2019). XRF technique. *Physical Sciences Reviews, 4*(8), 1–20. https://doi.org/10.1515/psr-2018-0171

Acquafredda, P., Larocca F., Muntoni, I. M., & Pallara, M. (2016). SEM and XRF analyses as a tool to discriminate obsidian provenance from archaeological sites of Central and Southern Italy. Paper presented at International Obsidian Conference (June 1-3 2016), Lipari (Italy).

Acquafredda, P., Andriani, T., Lorenzoni, S., & Zanettin, E. (1999). Chemical Characterization of Obsidians from Different Mediterranean Sources by Non-destructive SEM-EDS Analytical Method. *Journal of Archaeological Science, 26*(3), 315–325. https://doi.org/10.1006/jasc.1998.0372

Acquafredda, P., & Paglionico, A. (2004). SEM-EDS microanalyses of microphenocrysts of Mediterranean obsidians: a preliminary approach to source discrimination. *European Journal of Mineralogy, 16*(3), 419–429. https://doi.org/10.1127/0935-1221/2004/0016-0419

Acquafredda, P., & Muntoni, I. M. (2008). Obsidian from Pulo di Molfetta (Bari, Southern Italy): provenance from Lipari and first recognition of a Neolithic sample from Monte Arci (Sardinia). *Journal of Archaeological Science, 35*(4), 947–955. https://doi.org/10.1016/j.jas.2007.06.017

Acquafredda P., Mitolo D., & Muntoni I. M. (2011). Provenienza di ossidiana di Selva dei Muli (Frosinone), *Origini*, XXXIII, 233–236.

Acquafredda P., Muntoni I. M., & Pallara M. (2013). SEM-EDS and XRF characterization of obsidian bladelets from Portonovo (AN) to identify raw material provenance, *Origini*, XXXV, 69–82.

Acquafredda, P., & Larocca, F. (2017). Caratterizzazione archeologica e petrografica di manufatti neolitici dalla Grotta di Santa Barbara (Polignano a Mare - Bari). In F. Radina (Ed.), *Preistoria e Protostoria della Puglia, Studi di Preistoria e Protostoria* (Vol. 4, pp. 780–783). Firenze, Italy: Istituto Italiano di Preistoria e Protostoria.

Acquafredda, P., Muntoni, I. M., & Pallara, M. (2017). La provenienza dell'ossidiana nel Neolitico della Puglia. In F. Radina (Ed.), *Preistoria e Protostoria della Puglia, Studi di Preistoria e Protostoria* (Vol. 4, pp. 809–814). Firenze, Italy: Istituto Italiano di Preistoria e Protostoria.

Acquafredda, P., Muntoni, I. M., & Pallara, M. (2018). Reassessment of WD-XRF method for obsidian provenance shareable databases. *Quaternary International, 468*, 169–178. https://doi.org/10.1016/j.quaint.2017.08.020

Bellot-Gurlet, L., Le Bourdonnec, F., Popeau, G., & Dubernet, S. (2004). Raman microspectroscopy of Western Mediterranean obsidian glass: one step towards provenance study? *Journal of Raman Spectroscopy, 35*(89), 671–677. https://doi.org/10.1002/jrs.1195

Bigazzi, G., Bonadonna, F. P., Belluomini, G., & Malpieri, L. (1971). Studi sulle ossidiane italiane. IV. Datazione con il metodo delle tracce di fissione. *Bollettino della Società Geologica Italiana, 90*, 469–480.

Cann, J. R., & Renfrew, C. (1964). The characterisation of obsidian and its application to the Mediterranean region. *Proceedings of the Prehistoric Society, 30*, 111–133. https://doi.org/10.1017/S0079497X00015097

Carter, T., & Kilikoglou, V. (2007). From Reactor to Royalty? Aegean and Anatolian Obsidians from Quartier Mu, Malia (Crete). *Journal of Mediterranean Archaeology, 20*(1), 115–143. https://doi.org/10.1558/jmea.v20i1.115

De Francesco, A. M., Crisci, G. M., & Bocci, M. (2008). Non-destructive analytic method using XRF for determination of provenance of archaeological obsidian artefacts from the Mediterranean area: A comparison with traditional XRF methods. *Archaeometry, 50*(2), 337–350. https://doi.org/10.1111/j.1475-4754.2007.00355.x

De Francesco, A. M., Bocci, M., & Crisci, G. M. (2011). Non-destructive applications of wavelength XRF in obsidian studies. In M. S. Shackley (Ed.), *X-Ray Fluorescence Spectrometry (XRF) in Geoarchaeology* (pp. 81–107). New York: Springer. https://doi.org/10.1007/978-1-4419-6886-9_5

Duttine, M., Villeneuve, G., Poupeau, G., Rossi, A. M., & Scorzelli, R. B. (2003). Electron spin resonance of Fe^{3+} ion in obsidians from Mediterranean islands. Application to provenance studies. *Journal of Non-Crystalline Solids, 323*(1-3), 193–199. https://doi.org/10.1016/S0022-3093(03)00306-5

Frahm, E., Doonan, R. C. P., & Kilikoglou, V. (2014). Handheld portable X-ray fluorescence of Aegean obsidians. *Archaeometry, 56*(2), 228–260. https://doi.org/10.1111/arcm.12012

Freund, K. P. (2018). A long-term perspective on the exploitation of Lipari obsidian in central Mediterranean prehistory. *Quaternary International, 468*, 109–120. https://doi.org/10.1016/j.quaint.2017.10.014

Freund, K. P., & Tykot, R. H. (2011). Lithic technology and obsidian exchange networks in Bronze Age Nuragic Sardinia (Italy). *Archaeological and Anthropological Sciences, 3*(2), 151–164. https://doi.org/10.1007/s12520-010-0047-7

Gastaldi, P. (1974). Polla. In G. Bailo Modesti, B. d'Agostino, & P. Castaldi (Eds.), *Seconda Mostra della Preistoria e della Protostoria nel Salernitano* (pp. 51–66). Salerno: Ed. Laveglia.

Gordus, A. A., Wright, G. A., & Griffin, J. B. (1968). Obsidian Sources Characterized by Neutron-Activation Analysis. *Science, 161*(3839), 382–384. https://doi.org/10.1126/science.161.3839.382 PMID:17776740

Gratuze, B. (1999). Obsidian characterization by laser ablation ICP-MS and its application to prehistoric trade in the Mediterranean and the near east: Sources and distribution of obsidian within the Aegean and Anatolia. *Journal of Archaeological Science, 26*(8), 869–881. https://doi.org/10.1006/jasc.1999.0459

Larocca F. (2010). Grotta della Monaca: A prehistoric copper and iron mine in the Calabria region (Italy). In Anreiter P. et al. (Eds.), *Mining in european history and its impact on environment and human societies : proceedings for the 1st Mining in European History-Conference of the SFB-HIMAT, 12.-15. November 2009, Innsbruck* (pp. 267–270). Innsbruck: University Press.

Larocca, F. (2012). Grotta della Monaca (Calabria, Italia meridionale). Una miniera neolitica per l'estrazione dell'ocra. *Rubricatum. Revista del Museu de Gavà, 5*, 249–256.

Larocca, F. (2017). La Grotta di Santa Barbara a Polignano a Mare (Bari). Evidenze funerarie e cultuali di età neolitica. In F. Radina (Ed.), *Preistoria e Protostoria della Puglia, Studi di Preistoria e Protostoria* (Vol. 4, pp. 773–777). Firenze, Italy: Istituto Italiano di Preistoria e Protostoria.

Larocca, F., & Breglia, F. (2014). L'alta valle dell'Esaro e le sue miniere preistoriche. *Speleologia, 71*, 30–36.

Larocca, F., Minelli, A., & Larocca, A. (2019). Dentro la Pietra Sant'Angelo. Viaggio alla scoperta della preistoria nelle grotte di San Lorenzo Bellizzi. *Speleologia, 80*, 24–31.

Merrick, H. V., & Brown, F. H. (1984). Rapid chemical characterization of obsidian artefacts by electron microprobe analysis. *Archaeometry, 26*(2), 230–236. https://doi.org/10.1111/j.1475-4754.1984.tb00337.x

Minelli, A., & Larocca, F. (2019). Ricerche speleo-archeologiche nella Grotta di Polla (Salerno). *Speleologia, 80*, 18–19.

Nelson, D. E., D'Auria, J. M., & Bennett, R. B. (1975). Characterization of Pacific Northwest coast obsidian by X-ray fluorescence analysis. *Archaeometry, 17*(1), 85–97. https://doi.org/10.1111/j.1475-4754.1975.tb00117.x

Nielson, K. K., Hill, N. W., Mangelson, N. F., & Nelson, F. W. (1976). Elemental analysis of obsidian artefacts by proton particle induced X-ray emission. *Analytical Chemistry, 48*(13), 1947–1953. https://doi.org/10.1021/ac50007a035

Phillips, S. C., & Speakman, R. J. (2009). Initial source evaluation of archaeological obsidian from the Kuril Islands of the Russian Far East using portable XRF. *Journal of Archaeological Science, 36*(6), 1256–1263. https://doi.org/10.1016/j.jas.2009.01.014

Pouchou, J. L., & Pichoir, F. (1988). A simplified version of the "PAP" model for matrix corrections in EPMA. In Newbury D. E. (Ed.), *Microbeam Analysis* (pp. 315–318). San Francisco: San Francisco Press.

Pouchou, J. L., & Pichoir, F. (1991). Quantitative analysis of homogeneous or stratified microvolumes applying the model "PAP". In K. F. J. Heinrich & D. E. Newbury (Eds.), *Electron Probe Quantitation* (pp. 31–75). New York: Plenum Press. https://doi.org/10.1007/978-1-4899-2617-3_4

Shackley, M. S. (1998). Gamma rays, X-rays, and stone tools: Some current advances in archaeological geochemistry. *Journal of Archaeological Science, 25*(3), 259–270. https://doi.org/10.1006/jasc.1997.0247

Stewart, S. J., Cernicchiaro, G., Scorzelli, R. B., Poupeau, G., Acquafredda, P., & De Francesco, A. M. (2003). Magnetic properties and [57]Fe Mossbauer spectroscopy of Mediterranean prehistoric obsidians for provenance studies. *Journal of Non-Crystalline Solids, 323*(1-3), 188–192. https://doi.org/10.1016/S0022-3093(03)00305-3

Syvilay, D., Bousquet, B., Chapoulie, R., Orange, M., & Le Bourdonnec, F.-X. (2019). Advanced statistical analysis of LIBS spectra for the sourcing of obsidian samples. *Journal of Analytical Atomic Spectrometry, 34*(5), 867–873. https://doi.org/10.1039/C8JA00340H

Tykot, R. H., & Young, S.M. M. (1996). Archaeological applications of inductively coupled plasma-mass spectrometry. In Orna, M. V. (Ed.), *Archaeological Chemistry* (pp. 116–130), ACS Symposium Series 625. Washington, D.C.: American Chemical Society Library. https://doi.org/10.1021/bk-1996-0625.ch010

Tykot, R. H. (2017). Obsidian studies in the Prehistoric Central Mediterranean: After 50 years, what have we learned and what still needs to be done? *Open Archaeology, 3*(1), 264–278. https://doi.org/10.1515/opar-2017-0018

Wainwright, G. A. (1927). Obsidian. In Flinders Petries W. M. (Ed.) *Ancient Egypt* (pp. 77–93). British School of Archaeology in Egypt. London (UK): Macmillan Ltd.

Appendix

Table 1: WD-XRF detection of X-ray emission of some trace elements of the obsidian artefacts. The X-rays intensity values, expressed as counts per second, are background and interference free. Some characterizing ratios are also reported.

Grotta di Pietra Sant'Angelo (San Lorenzo Bellizzi - CS)

sample	Rb	Sr	Y	Zr	Nb	Zr/Y	Nb/Y	Rb/Sr	Nb/Sr
SLB7	3566.2	171.8	587.4	3179.0	669.1	5.41	1.14	20.76	3.90
SLB10	6757.4	384.4	1402.2	6339.1	1368.7	4.52	0.98	17.58	3.56
SLB13	4264.9	248.3	879.9	4185.0	926.4	4.76	1.05	17.18	3.73
SLB34	13050.5	695.8	2785.5	12355.7	2740.8	4.44	0.98	18.76	3.94
SLB35	3669.1	196.1	633.6	3324.8	701.6	5.25	1.11	18.71	3.58
SLB42a	2966.2	176.4	627.3	3064.0	663.0	4.88	1.06	16.82	3.76
SLB42b	1779.3	95.8	267.6	1643.1	348.3	6.14	1.30	18.58	3.64
SLB42c	2119.8	114.8	340.9	1916.8	403.7	5.62	1.18	18.47	3.52
SLB44	3282.1	165.2	638.2	3361.9	741.5	5.27	1.16	19.87	4.49
SLB45	4314.8	215.0	837.4	4029.8	859.6	4.81	1.03	20.07	4.00
SLB49	13792.6	756.6	2845.4	12459.4	2694.7	4.38	0.95	18.23	3.56
SLB50	11046.7	607.3	2291.7	9893.2	2153.9	4.32	0.94	18.19	3.55
SLB51	4557.9	239.3	875.4	4095.2	875.8	4.68	1.00	19.04	3.66
SLB52	13949.5	749.9	2890.4	12630.9	2739.8	4.37	0.95	18.60	3.65
SLB53	13073.0	735.3	2662.3	11859.4	2564.4	4.45	0.96	17.78	3.49
SLB58	12179.7	671.2	2544.7	11045.8	2423.8	4.34	0.95	18.15	3.61
SLB61a	2816.4	140.9	499.4	2681.3	576.5	5.37	1.15	19.99	4.09
SLB61b	4846.2	280.6	944.8	4519.5	974.5	4.78	1.03	17.27	3.47
SLB62	8260.6	431.4	1695.1	7704.7	1680.8	4.55	0.99	19.15	3.90
SLB63	4729.1	253.7	910.9	4318.2	905.1	4.74	0.99	18.64	3.57
SLB64	3987.8	228.3	822.7	3844.8	799.5	4.67	0.97	17.47	3.50
SLB77	5952.8	319.1	1229.1	5314.3	1170.6	4.32	0.95	18.65	3.67
SLB78	5022.7	249.3	963.9	4728.2	1038.2	4.91	1.08	20.15	4.16
SLB87a	9680.9	515.1	1972.3	8622.1	1868.2	4.37	0.95	18.79	3.63
SLB87b	1652.0	75.8	195.6	1475.9	293.3	7.55	1.50	21.79	3.87
SLB87c	1727.5	79.3	269.9	1729.0	370.4	6.41	1.37	21.78	4.67
SLB87d	1582.2	98.4	277.7	1602.8	324.5	5.77	1.17	16.07	3.30
SLB87e	2022.6	117.3	338.7	1861.2	373.7	5.49	1.10	17.24	3.19
SLB87f	2051.6	93.2	314.4	1885.2	377.5	6.00	1.20	22.01	4.05
SLB91	12894.3	713.8	2676.8	11537.9	2543.5	4.31	0.95	18.07	3.56
SLB93	9194.8	526.4	1976.1	8412.6	1822.2	4.26	0.92	17.47	3.46
SLB96	2522.1	137.3	481.3	2458.0	556.4	5.11	1.16	18.37	4.05
SLB114	3400.3	184.8	639.5	3188.3	657.5	4.99	1.03	18.40	3.56
SLB136	10258.4	563.6	2032.1	9098.1	1958.9	4.48	0.96	18.20	3.48
SLB142a	5543.2	296.4	1076.5	5109.6	1099.8	4.75	1.02	18.70	3.71
SLB142b	3030.0	165.8	590.5	2990.1	627.5	5.06	1.06	18.28	3.79
SLB208	1356.5	80.7	217.7	1371.6	275.1	6.30	1.26	16.82	3.41
SLB216	1135.4	58.0	107.0	1061.4	219.1	9.92	2.05	19.58	3.78

continued **Table 1**

SLB223	10759.7	580.4	2298.8	9862.7	2171.2	4.29	0.94	18.54	3.74
SLB230	1488.3	83.3	166.8	1288.8	239.8	7.72	1.44	17.86	2.88
SLB232	5881.7	333.2	1194.7	7504.7	1103.8	6.28	0.92	17.65	3.31
SLB238	7646.5	414.3	1554.5	7056.9	1508.9	4.54	0.97	18.46	3.64
SLB240	2241.0	123.8	396.0	2133.6	450.5	5.39	1.14	18.10	3.64
SLB282	1890.5	90.0	316.4	2010.5	391.2	6.35	1.24	21.00	4.35
SLB293	4110.1	233.0	811.5	3899.9	824.2	4.81	1.02	17.64	3.54
SLB294	4288.6	228.1	851.9	4143.4	880.5	4.86	1.03	18.80	3.86

Grotta del Tesauro (Sant'Agata Di Esaro - CS)

sample	Rb	Sr	Y	Zr	Nb	Zr/Y	Nb/Y	Rb/Sr	Nb/Sr
GdT5	8642.7	486.2	1660.1	7767.7	1655.6	4.68	1.00	17.78	3.41
GdT6	16106.3	912.8	3282.3	14620.0	3201.6	4.45	0.98	17.64	3.51
GdT7	10491.0	567.9	2145.2	9490.4	2085.5	4.42	0.97	18.47	3.67
GdT8	7144.6	572.0	1376.2	6479.2	1396.1	4.71	1.01	12.49	2.44
GdT9	10243.4	720.9	2039.1	9034.8	1956.8	4.43	0.96	14.21	2.71
GdT10	9766.0	591.0	1999.3	8878.6	1999.0	4.44	1.00	16.53	3.38
GdT11	3449.6	201.4	671.2	3311.1	718.1	4.93	1.07	17.12	3.56
GdT12	16085.4	1130.1	3340.1	14875.6	3307.6	4.45	0.99	14.23	2.93
GdT12A	3436.6	233.5	716.0	3144.6	710.5	4.39	0.99	14.72	3.04
GdT12B	2368.7	137.2	397.4	2163.3	433.8	5.44	1.09	17.26	3.16
GdT13	13765.2	764.6	2831.5	12551.0	2789.4	4.43	0.99	18.00	3.65

Grotta di Polla (Polla - SA)

sample	Rb	Sr	Y	Zr	Nb	Zr/Y	Nb/Y	Rb/Sr	Nb/Sr
Polla1	2545.9	125.2	400.3	2417.8	476.0	6.04	1.19	20.33	3.80
Polla2	16166.0	897.9	3455.6	14824.9	3222.2	4.29	0.93	18.01	3.59
Polla3	11207.6	637.3	2419.1	10589.0	2300.0	4.38	0.95	17.58	3.61
Polla4	8492.9	432.9	1589.2	7598.3	1622.3	4.78	1.02	19.62	3.75
Polla5	18253.4	961.9	3790.7	16596.6	3522.7	4.38	0.93	18.98	3.66

Table 2: SEM-EDS microanalyses of the glass of the obsidian artefacts; each value reported in the table represents the mean of three different determinations. C.I.A. = Chemical Index of alteration [$Al_2O_3/(Al_2O_3 + CaO + Na_2O + K_2O)$ in mol.%].

Grotta della Monaca (Sant'Agata Di Esaro - CS)

sample	SiO_2	Al_2O_3	FeO	MgO	CaO	Na_2O	K_2O	CIA	
GdM11	74.87	13.43	1.33	0.12	0.58	4.39	5.28	48.98	
GdM12	74.69	13.27	1.44	0.27	0.64	3.70	5.99	49.14	
GdM13	74.63	13.65	1.35	0.18	0.66	4.40	5.13	49.38	
GdM14	74.33	13.23	1.48	0.16	0.68	3.96	6.16	47.85	
GdM15	74.62	13.32	1.49	0.17	0.63	4.40	5.38	48.39	
GdM17	74.53	13.46	1.37	0.24	0.68	4.35	5.37	48.65	
GdM18	74.70	13.54	1.38	0.25	0.74	3.98	5.40	49.64	
GdM19	73.15	13.13	1.42	0.69	0.55	4.66	6.41	45.70	
GdM20	73.84	13.07	1.43	0.64	0.63	4.79	5.60	46.42	
GdM21	73.90	13.18	1.25	0.74	0.52	5.17	5.24	46.57	
GdM22	74.17	13.01	1.43	0.68	0.56	4.00	6.15	47.72	
GdM23	73.26	13.07	1.50	0.61	0.61	5.41	5.54	44.95	
GdM98	74.31	13.40	1.26	0.30	0.53	3.91	6.30	48.53	
GdM133	74.26	13.38	1.54	0.24	0.60	4.12	5.86	48.49	
GdM140	74.68	13.29	1.33	0.26	0.58	4.22	5.63	48.54	
GdM142	74.58	13.20	1.39	0.28	0.63	3.98	5.94	48.31	
GdM143	74.60	13.22	1.42	0.27	0.57	4.35	5.57	48.18	
GdM144	74.37	13.25	1.53	0.26	0.57	3.81	6.21	48.58	
GdM145	74.54	13.25	1.38	0.29	0.56	3.89	6.10	48.59	
GdM147	74.51	13.18	1.57	0.23	0.60	3.91	6.00	48.46	
GdM149	74.51	13.19	1.41	0.28	0.64	3.89	6.08	48.26	
GdM150	74.70	13.27	1.34	0.28	0.52	3.52	6.37	49.33	
GdM152o	67.49	12.11	1.83	0.25	2.00	11.29	5.04	30.45	*
GdM152p	69.20	12.51	1.39	0.26	1.41	9.74	5.49	33.78	**
GdM152g	74.41	13.28	1.42	0.26	0.59	5.00	5.04	47.37	***
GdM154	74.20	13.51	1.32	0.27	0.57	4.35	5.81	48.27	
GdM155	74.62	13.12	1.43	0.20	0.59	3.71	6.33	48.33	
GdM158	74.96	13.01	1.34	0.24	0.61	3.74	6.10	48.41	
GdM159	74.68	13.31	1.35	0.23	0.57	4.19	5.67	48.62	
GdM160	74.50	13.27	1.35	0.24	0.57	4.20	5.86	48.15	
GdM162	74.67	13.14	1.50	0.17	0.66	3.51	6.35	48.69	
GdM163o	68.52	12.18	1.39	0.32	0.93	10.99	5.67	31.98	*
GdM163p	67.92	12.12	1.38	0.35	1.14	12.35	4.73	30.58	**
GdM163g	74.12	13.55	1.27	0.32	0.59	5.14	5.02	47.52	***
GdM164	74.57	13.34	1.38	0.20	0.53	4.26	5.71	48.52	
GdM166	73.89	13.17	1.40	0.29	0.50	4.05	6.70	47.05	
GdM167	74.79	13.23	1.33	0.22	0.62	3.71	6.11	48.87	
GdM72n	74.35	13.49	1.36	0.29	0.61	4.87	5.03	48.08	

*untreated sample; **after 72 hours of acetic acid treatment; ***cutted fresh surface

Table 2

Grotta di Polla (Polla - SA)

sample	SiO$_2$	Al$_2$O$_3$	FeO	MgO	CaO	Na$_2$O	K$_2$O	CIA
Polla6	75.39	12.89	1.52	0.00	0.80	4.09	5.28	48.12

Grotta di Santa Barbara (Polignano a Mare - BA)

sample	SiO$_2$	Al$_2$O$_3$	FeO	MgO	CaO	Na$_2$O	K$_2$O	CIA	
GSB3	74.30	13.38	1.34	0.28	0.70	4.91	4.98	47.58	
GSB4	74.82	13.23	1.33	0.28	0.58	4.54	5.14	48.43	
GSB6	74.84	13.18	1.53	0.24	0.64	4.16	5.34	48.87	
GSB7	74.64	13.25	1.56	0.22	0.60	4.37	5.35	48.50	
GSB12	74.50	13.41	1.35	0.28	0.61	4.64	5.12	48.42	
GSB13	74.76	13.20	1.58	0.29	0.66	3.95	5.49	49.18	
GSB17	74.79	13.51	1.15	0.29	0.59	4.74	4.88	48.84	
GSB19	74.50	13.44	1.35	0.33	0.64	4.61	5.03	48.64	
GSB23	74.54	13.32	1.38	0.24	0.55	4.76	5.10	48.14	
GSB24	74.72	13.25	1.34	0.25	0.66	4.62	5.07	48.12	
GSB25	74.53	13.37	1.40	0.24	0.64	4.54	5.19	48.41	
GSB26	74.88	13.15	1.47	0.24	0.66	4.12	5.41	48.73	
GSB27	74.62	13.25	1.49	0.26	0.64	4.58	5.11	48.22	
GSB28o	74.76	14.04	0.58	0.33	0.54	5.69	3.96	48.97	*
GSB28p	74.64	13.21	1.50	0.22	0.65	4.47	5.24	48.18	**
GSB31	73.85	13.26	1.41	0.32	0.60	3.52	6.98	47.88	
GSB32	74.25	13.13	1.58	0.30	0.57	3.76	6.32	48.29	
GSB37	74.51	13.28	1.57	0.28	0.64	4.37	5.25	48.62	
GSB38	74.95	13.29	1.58	0.29	0.74	3.93	5.19	49.74	
GSB39	75.03	13.06	1.63	0.19	0.64	3.75	5.64	49.29	
GSB40	74.65	13.22	1.49	0.25	0.63	4.49	5.20	48.28	
GSB41	74.96	13.02	1.51	0.22	0.64	4.22	5.37	48.33	
GSB42	74.87	13.12	1.49	0.25	0.61	4.35	5.28	48.41	
GSB45	74.64	13.32	1.44	0.22	0.63	4.51	5.18	48.45	
GSB49	74.51	13.34	1.38	0.25	0.57	4.77	5.17	47.95	
GSB51	74.82	13.08	1.61	0.30	0.65	4.00	5.44	48.93	
GSB53	75.17	13.28	1.59	0.27	0.67	3.70	5.23	50.60	
GSB54	74.45	13.12	1.53	0.25	0.63	4.36	5.54	47.82	
GSB59	74.90	13.18	1.36	0.27	0.62	4.19	5.42	48.70	
GSB60	74.91	13.07	1.65	0.27	0.69	3.77	5.56	49.24	
GSB67	74.60	13.34	1.47	0.28	0.67	4.16	5.36	49.04	
GSB68	74.55	13.27	1.43	0.26	0.60	4.63	5.19	48.09	
GSB71	74.67	13.31	1.42	0.23	0.67	4.36	5.28	48.55	
GSB73	74.49	13.34	1.51	0.25	0.65	4.51	5.21	48.37	
GSB74	74.66	13.27	1.36	0.27	0.63	4.60	5.14	48.17	
GSB103	74.38	13.53	1.20	0.29	0.61	5.20	4.67	47.90	

Table 2

sample	SiO$_2$	Al$_2$O$_3$	FeO	MgO	CaO	Na$_2$O	K$_2$O	CIA	
GSB110	74.65	13.24	1.47	0.27	0.65	4.30	5.33	48.56	
GSB115	74.44	13.39	1.40	0.29	0.67	4.60	5.11	48.33	
GSB116	74.52	13.27	1.46	0.28	0.67	4.57	5.15	48.11	
GSB117	74.82	13.27	1.33	0.24	0.63	4.10	5.51	48.92	
GSB120	74.68	13.26	1.49	0.25	0.62	4.50	5.08	48.59	
GSB126	73.90	13.35	1.37	0.26	0.52	4.30	6.17	47.60	
GSB127	74.59	13.26	1.42	0.28	0.66	4.47	5.23	48.26	
GSB130	74.64	13.38	1.31	0.27	0.49	4.83	5.01	48.41	
GSB131	74.89	13.12	1.59	0.29	0.67	4.05	5.27	49.13	
GSB132	74.54	13.29	1.44	0.29	0.61	4.32	5.42	48.55	
GSB133o	74.32	13.82	1.21	0.34	0.22	4.37	5.65	50.21	*
GSB133p	74.18	13.35	1.31	0.18	0.29	4.90	5.68	47.53	**
GSB138	74.74	13.21	1.53	0.27	0.66	4.23	5.29	48.76	
GSB140	74.39	13.45	1.29	0.27	0.64	4.94	4.95	47.87	
GSB142	74.44	13.39	1.41	0.29	0.58	4.78	5.04	48.23	
GSB145	74.91	13.16	1.45	0.26	0.68	4.14	5.36	48.73	
GSB149	74.71	13.03	1.66	0.26	0.70	3.95	5.59	48.53	
GSB153	74.85	13.52	1.11	0.24	0.59	4.82	4.82	48.74	
GSB154	74.59	13.24	1.52	0.25	0.62	4.47	5.17	48.47	
GSB155	74.40	13.44	1.39	0.27	0.60	4.92	4.89	48.14	

*untreated sample; **after 12 days of acetic acid treatment

Table 3: Mean of 10 microanalyses on two reference standards (Augite and Orthoclase) with the relative standard deviation (σ) and the certified value from Micro-Analysis Consultants Ltd. (U.K.); n.d. = not detected.

Augite	mean	σ	certified value
SiO$_2$	46.27	0.10	45.93
TiO$_2$	2.39	0.05	2.29
Al$_2$O$_3$	8.76	0.08	9.02
Cr$_2$O$_3$	n.d.	---	0.08
FeO	7.21	0.08	7.42
MnO	0.06	0.06	0.07
MgO	12.07	0.08	11.88
CaO	21.80	0.07	21.62
Na$_2$O	0.85	0.06	0.79
K$_2$O	n.d.	---	0.01
Tot.	99.41		99.11

Orth.	mean	σ	certified value
SiO$_2$	64.07	0.11	64.30
Al$_2$O$_3$	20.02	0.08	19.90
CaO	0.18	0.04	0.24
Na$_2$O	3.86	0.04	3.70
K$_2$O	11.37	0.06	11.40
Tot.	99.50		99.54